Atmos. Chem. Phys. Discuss., https://doi.org/10.5194/acp-2017-855
Manuscript under review for journal Atmos. Chem. Phys.
Discussion started: 27 October 2017

Effect of ecological restoration programs on dust pollution in North China Plain: a case study

Xin Long[1,2], Xuexi Tie[1,2,3,4,5*], Guohui Li[1,2*], Junji Cao[1,2], Tian Feng[1,6], Li Xing[1,2], Zhisheng An[2]

[1]Key Laboratory of Aerosol Chemistry and Physics, Institute of Earth Environment, Chinese Academy of Sciences, Xi'an 710061, China

[2]State Key Laboratory of Loess and Quaternary Geology, Institute of Earth Environment, Chinese Academy of Sciences, Xi'an 710061, China

[3]Center for Excellence in Urban Atmospheric Environment, Institute of Urban Environment, Chinese Academy of Sciences, Xiamen 361021, China

[4]Shanghai Key Laboratory of Meteorology and Health, Shanghai, 200030, China

[5]National Center for Atmospheric Research, Boulder, CO 80303, USA

[6]Xi'an AMS Center, Xi'an 710061, China

Correspondence and requests for materials should be addressed to:

Xuexi Tie (email: xxtie@ucar.edu) *and* Guohui Li (email: ligh@ieecas.cn)

Abstract: In recent years, Chinese government has taken great efforts in initiating large-scale ecological restoration programs (ERPs) to reduce the dust pollutions in China. Using a satellite measurement product of Moderate Resolution Imaging Spectroradiometer (MODIS), the changes in land cover are quantitatively evaluated in this study. We find that grass and forest are increased in berried lands and deserts in northwestern China, which locate in the upwind regions of the populated areas of the North China Plain (NCP) in eastern China. As a result, the changes in land cover could produce important impacts on the dust pollutions in eastern of China. To assess the effect of ERPs on dust pollutions, a regional transport/dust model (WRF-DUST, Weather Research and Forecast model with dust) is applied to investigate the evolution of dust pollutions during a strong dust episode (from 2 to 8 March 2016). The calculations are intensively evaluated by comparing with the measured data. Despite some model biases, the WRF-DUST model reasonably reproduced the temporal variations and spatial distributions during the dust storm event. The correlation coefficient (R) between the calculated and measured dust concentrations is 0.77. The indices of agreement (IOAs) are 0.96 and 0.83, and the normalized mean bias (NMBs) are 2% and -15% in the dust source region (DSR) and the downwind populated area of NCP, respectively, suggesting that the WRF-DUST model well captures the spatial variations and temporal evolutions of the dust storm event. The impacts of EPRs induced land cover changes on the dust pollutions in NCP are quantitatively assessed using the WRF-DUST model. We find that the ERPs significantly reduce the dust pollutions in NCP, especially in the heart area of NCP (BTH, Beijing-Tianjin-Hebei). During the episode when the dust storm was transported from the DSR to NCP, the reduction of dust pollutions induced by ERPs ranges from -5% to -15% in NCP, with the maximum reduction of -15.3% (-21.0 μg m^{-3}) in BTH, and -6.2% (-9.3 μg m^{-3}) in NCP. Because the air pollution is severe in eastern China, especially in NCP, the reduction of dust pollutions has important effects on the severe air pollutions. This study shows that ERPs help to reduce air pollutions in the region, especially in springtime, suggesting the important contributions of ERPs to the air pollution control in China.

Key words: Ecological restoration programs; Dust pollution; North China Plain; WRF-DUST

1 Introduction

Dust particles have wide impacts on the Earth's radiative forcing budget (Liao et al., 2004; Haywood et al., 2005), cloud formation (Rosenfeld et al., 2001), atmospheric dynamics (Evan et al., 2008), air quality (Giannadaki et al., 2014), and ocean biogeochemistry (Jickells et al., 2005) in various spatial and temporal scales. Distinguished from the increasing trends observed in other major dust source regions (Moulin et al., 1997), the East Asian dust storms are in decreasing trends since 1950s except for a spike in dust activity (Lee and Sohn, 2011; Wang et al., 2017). The East Asian dust storms could be transported to southern/eastern China (Qian et al., 2002), Korea (Park and In, 2003), and Japan (Watanabe et al., 2014) and even the west coast of North America (Cottle et al., 2013; Yoon et al., 2017). There are two dominant source regions of East Asian dust storms locate in China, including the Taklamakan Desert in northwest China and the Gobi Desert in Mongolia and northern China (Sun et al., 2005; Wang et al., 2011). Along the transport pathway, mineral dust particles lead to significant impacts on human's life in the densely populated areas of southern/eastern part of China (Bian et al., 2011; Zhao et al., 2013).

To reduce dust pollution problem and to improve the environmental conditions, the Chinese government has taken great efforts in initiating large-scale ecological restoration programs (ERPs) (Yin and Yin, 2010; Cao et al., 2011). Chinese ERPs are among the biggest programs in the world because of their ambitious goals, massive scales, huge payments and potentially enormous impacts. As a result, the "Green Wall of China" has been established in North China (Duan et al., 2011). There are strong evidences that a remarkable vegetation increase trend has occurred in the dominant dust source areas, northwestern China, especially after 2000 (Piao et al., 2003; Peng et al., 2011). And the dust storm frequency in Northern China is generally in decreasing trends (Li et al., 2014; Wang et al., 2007). However, it is still prevalent the ongoing debate about effectiveness of the national ERPs. Numerous experts and government officials have attributed the decrease trend to the success of ERPs in controlling dust storms and combated desertification (Wang et al., 2007; Liu et al., 2008; Tan and Li, 2015). Conversely, several experts have doubted the program's effectiveness (Jiang, 2005; Wang et al., 2010; Cao et al., 2011), generally asserting the climate factors being the main cause for the observed decrease of dust storms in northern China (Li et al., 2014; Fan et al., 2017). Some experts further highlight the potential deterioration of the ecosystem with severe depletion of soil moisture, especially in semiarid and arid regions (Deng et al., 2016; Lu et al., 2016). Hence, there is an increasing need to evaluate the China's ERPs at controlling dust pollution, particularly for the downwind densely populated areas, to improve the decision support for ecological planning and implementation. The mineral dust particles can also serve as carriers and reaction platforms, and the heterogeneous dust chemistry may change the photochemistry, acid deposition, and production of secondary aerosols in the atmosphere (Lou et al., 2014; Fu, 2016; Zhou et al., 2016). The rigorous evaluation of ecological efforts is also beneficial to improve the understanding of the attractive haze pollution research in NCP.

There are difficulties to estimate the effectiveness of ERPs in dust control, which are seldom quantitatively specified. On one hand, it is hard to quantify the influence of ERPs in regional scale. The vegetation indices (e.g. NDVI, normalized-difference vegetation index) are the most utilized parameters to conduct quantitative evaluation of ERPs' effectiveness (Duan et al., 2011; Lü et al., 2015; Tan and Li, 2015). But the vegetation indices are not efficient indicators for dust emission, which are mainly related to erodibility of barren land surface directly (Bian et al., 2011). On the other hand, it is hard to distinguish the influences of climate factors, which have been generally asserted to be one of the main causes for the observed decrease of dust storms in northern China. To exclude the influences of climate factors, Tan and Li (2015) have compared the correlation of dust storm indices (intensity and frequency), NDVI, wind speed, and precipitation within and outside the "Green Great Wall" regions, qualitatively inferring the effectiveness of ERPs in reducing dust storm intensity. However, the previous studies didn't quantify the roles of ERPs, such as the detailed variations of ERPs, the effect of regional transport to downwind regions, etc. The focus of our work is to use detailed satellite measurements to assess the region of ERPs, and to use a regional model to quantify the effect of ERPs on the downwind regions, especially in the NCP region.

Here our narrative is independently based on first-hand sources of satellite measurements and WRF-DUST model simulation. We investigated the ERPs induced land cover changes in China using the long-term MODIS land cover products. The

Atmos. Chem. Phys. Discuss., https://doi.org/10.5194/acp-2017-855
Manuscript under review for journal Atmos. Chem. Phys.
Discussion started: 27 October 2017

impacts of the ERPs induced land cover changes on the dust pollution in NCP were further quantitatively evaluated using the WRF-DUST model. We selected two regions of interest (ROIs) (**Fig. 1**): (1) the polluted and dense populated downwind areas of dust storms, the North China Plain (NCP), including five provinces of the Beijing, Tianjin, Hebei, Henan and Shandong; (2) the dust source region and surrounding areas (DSR), including five provinces in the northwest of NCP (Ningxia, Gansu, Shanxi, Inner Mongolia and Shanxi). The details of ROIs are shown in **Fig. 1b**. The methodology and WRF-DUST model configuration are described in Sect. 2. Data analysis and model results are presented in Sect. 3, together with the conclusions and discussions in Sect. 4.

2 Model and methodology

2.1 Dust pollutants measurements

The China Ministry of Environmental Protection (China MEP) has commenced to release real-time hourly observations of pollutants since 2013, including O_3, NO_2, CO, SO_2, $PM_{2.5}$, and PM_{10} (particulate matter with aerodynamic diameter less than 2.5 and 10 μm, respectively). We collected the hourly near-surface $PM_{2.5}$ and PM_{10} mass concentrations from the China MEP (http://www.aqistudy.cn/). Because there are no detailed aerosol compositions measurements, the $PM_{2.5\text{-}10}$ (particulate matter with aerodynamic diameter between 2.5 and 10 μm) mass concentrations (defined as "[PMC]" in the later discussion) were utilized to analyze the dust pollution events. According to several previous studies, the use of [PMC] also has two advantages: (1) the size distribution of dust mass is center on the coarse model, and (2) the difference between PM_{10} and $PM_{2.5}$ can effectively decrease the uncertainty of anthropogenic fine particulate matter, such as sulfate, nitrate, and organic aerosols (Ho et al., 2003; Shen et al., 2011). A total of 184 cities (489 measurement sites) had [PMC] observations in the research domain, including 30 cities within the DSR region and 53 cities within the NCP region (**Fig. 1a**). Because the prevailing winds were dominated by west winds, the most measurement sites (as shown in **Fig. 1a**) locate in the downwind area of the dust source regions (such as barren lands and deserts). As a result, the China MEP measurement network provides a good opportunity to explore

Atmos. Chem. Phys. Discuss., https://doi.org/10.5194/acp-2017-855
Manuscript under review for journal Atmos. Chem. Phys.
Discussion started: 27 October 2017

Atmospheric Chemistry and Physics
Open Access
Discussions

the dust pollution evolution.

2.2 MCD12Q1 data assimilation and land cover changes assessment

We quantitatively evaluated the characteristics of annual land cover using the MODIS land cover products (MCD12Q1), derived from the Terra- and Aqua- Moderate Resolution Imaging Spectroradiometer (MODIS) observations (Friedl et al., 2002). The MCD12Q1 have been widely used in studies of atmospheric science, hydrology, ecology, and land change science (Gerten et al., 2004; Guenther, 2006; Reichstein et al., 2007; Turner et al., 2007). The IGBP (International Geosphere Biosphere Programme) classification within MCD12Q1 (Version 5.1) was analyzed to explore the variability of the land use fraction (LUF) from 2001 to 2013. The IGBP layer is generated using a supervised classification algorithm in conjunction with a revised database of high quality land cover training sites (Friedl et al., 2010). Its accuracy is estimated to be 72.3-77.4% (average 75%) globally, with a 95% confidence interval (Friedl et al., 2002; Friedl et al., 2010).

The IGBP layer in MCD12Q1 is well consistent with the MODIS land use scheme in the WRF-CHEM model, including 11 natural vegetation classes, 3 developed and mosaicked land classes, and 3 non-vegetated land classes. **Supplementary Table 1** shows the land use categories for the WRF-CHEM MODIS data and MCD12Q1. We conducted the geospatial processing to assimilate the MCD12Q1 data (500 m) to fit in the WRF-CHEM model (9 km in the present study) by the following steps. (1) Convert the original raster MCD12Q1 dataset to vector files (esri-shapefile) and re-projected them based on the geographic coordinate system configurations in WRF-CHEM module (Its pre-processors). (2) Create vector files (shapefile) of each grid based the domain of WRF-CHEM. (3) Access and iterate the selected grid-shapefile to partition the converted the MCD12Q1 vector dataset into model resolution using the Esri ArcGIS library (arcpy). The empty grids were populated with the vector MCD12Q1 dataset using a spatial join operation in ArcGIS, joining one input feature to one output feature (no aggregation) whenever input and output polygon features intersect. This methodology preserves the values of the original MCD12Q1 dataset. (4) Transcribe the newly merged and re-gridded MCD12Q1 datasets into text files readable in WRF-CHEM pre-processors, calculating the

Atmos. Chem. Phys. Discuss., https://doi.org/10.5194/acp-2017-855
Manuscript under review for journal Atmos. Chem. Phys.
Discussion started: 27 October 2017

gridded LUF of each category by

$$LUF_{i,j,k} = \frac{Area_{i,j,k}}{Area_{i,j}} \quad (1)$$

where i and j are grid indices, $Area_{i,j,k}$ stands for the total area of each land use category k within grid cell (i, j), and $Area_{i,j}$ is the area of grid cell (i, j). The $LUF_{i,j,k}$ ranges from 0 to 1, representing the emission potential of the specified dust source (k) in each grid cell (i, j). The larger $LUF_{i,j,k}$, the higher dust emission potential.

2.3 WRF-DUST model and configurations

In the present study, we utilized a specific WRF-DUST model developed based on a regional chemical model WRF-CHEM (version 3.2) (Grell et al., 2005). The GOCART (Georgia Tech/Goddard Global Ozone Chemistry Aerosol Radiation and Transport model) scheme (Chin et al., 2000) was utilized to calculate the physical processes of dust emission, transport, dry depositions, and gravitational settling. The dust particle sizes are divided into five size bins with effective radius of 0.7, 1.4, 2.4, 4.5 and 8.0 μm. The dust emission in each dust size bins is size-resolved. Dust emission is dependent on the surface wind velocity (Ginoux et al., 2001), and surface land cover properties (such as soil composition, vegetation, soil moisture content, and soil erodibility) (Grini et al., 2005; Li et al., 2016a), which can be calculated by

$$G_p = \begin{cases} C\gamma_p E V^2 \left(V - Vt_p\right) & V > Vt_p \\ 0 & V \leq Vt_p \end{cases} \quad (2)$$

Where G is the dust emission flux (kg s^{-1}); p is the dust size bin; C is a dimensional factor (0.8 μg s^2 m^{-5}); γ is the dust particle fraction; E is the probability soil erosion factor; V is the near-surface wind velocity at 10 m (m s^{-1}); and Vt is the threshold velocity (m s^{-1}).

The WRF- DUST model was applied to simulate dust storm events in several previous studies (Kang et al., 2009; Bian et al., 2011; Wang et al., 2012; Li et al., 2016a). These studies reported that the WRF-DUST model is generally capable of simulating dust storm events in the Asian region.

Because the dust emissions are strongly dependent on different categories of land cover, to better investigate the impacts of land cover changes on the dust emission, we modified the GOCART dust emission scheme, considering the each land cover dust source categories other than the dominant category. The flux of dust emission G in each grid is given by

$$G_p = \begin{cases} \sum_k LUF_k C \gamma_p E V^2 (V - V\square_p) & V > Vt_p \\ 0 & V \leq Vt_p \end{cases} \quad (3)$$

LUF_k denotes the gridded area fraction of land cover category k derived from the satellite data (MCD12Q1) assimilation. The other parameters are the same as those in Eq. (2). We set the erosion factor E=0.12 for cropland and E=0.5 for barren following the previous studies.

A dust storms episode from 2 to 8 March 2016 in northern China was simulated using the WRF-DUST model. The WRF-DUST model adopts one grid with horizontal resolution of 9 km centered in (112°E, 41°N) and 35 sigma levels in the vertical direction. The grid cells used for the domain are 500×300 (**Fig. 1**). The physical parameterizations include the microphysics scheme of Hong and Lim (2016), the Mellor–Yamada–Janjic (MYJ) turbulent kinetic energy (TKE) planetary boundary layer scheme (Janić, 2001), the unified Noah land-surface model (Chen and Dudhia, 2001). Meteorological initial and boundary conditions were taken from the 1°×1° reanalysis data of National Centers for Environmental Prediction (NCEP). For the episode simulations, the spin-up time is 3 days. Considering the impacts of the local dust emission, the coarse mode of anthropogenic particulate matter emission was included in the calculation. The detailed emission inventory was obtained from the Multi-resolution Emission Inventory for China (MEIC) (Zhang et al., 2009), which is then updated and improved for the year 2010 (http://www.meicmodel.org).

2.4 Statistical methods for comparisons

In order to assess the effect of the ERPs induced land cover changes on the dust pollutions in China, the model calculation is statistically evaluated. The following statistical parameters are calculated for evaluating the model calculation, including the normalized mean bias (*MB*), the index of agreement (*IOA*), and the correlation coefficient (R). These parameters are utilized to assess the WRF-CHEM model performance in simulating air pollutants against measurements.

$$NMB = \frac{\sum_{i=1}^{N}(P_i - O_i)}{\sum_{i=1}^{N} O_i} \quad (4)$$

$$IOA = 1 - \frac{\sum_{i=1}^{N}(P_i - O_i)^2}{\sum_{i=1}^{N}(|P_i - \bar{O}| + |O_i - \bar{O}|)^2} \quad (5)$$

$$R = \frac{\sum_{i=1}^{N}(P_i - \bar{P})(O_i - \bar{O})}{[\sum_{i=1}^{N}(P_i - \bar{P})^2 \sum_{i=1}^{N}(O_i - \bar{O})^2]^{\frac{1}{2}}} \quad (6)$$

where P_i and O_i are the calculated and observed PMC concentrations ([PMC]), respectively. *N* is the total number of the predictions used for comparisons, and $\bar{O}$ represents the average of the prediction and observation, respectively. The *IOA* ranges from 0 to 1, with 1 showing perfect agreement of the prediction with the observation. The *R* ranges from -1 to 1, with 1 implicating perfect spatial consistency of observation and prediction.

3 Results and discussions

3.1 Land Cover change induced by ERPs

The land surface changes due to the ecological restoration programs (ERPs) were assessed using the MCD12Q1 product. From 2001 to 2013, the land cover exhibits two obvious vegetation increase trends between the dust source region in northwester China and dense populated areas in eastern China. Firstly, there is a regional grass/savanna increase trend with obvious LUF increase of grass/savanna categories (**Fig. 2b**), corresponding with a regional LUF decrease in barren categories in northwestern China (**Fig. 2a**). The result is consistent with the previous research based on long-term official and synthesized data, which also found a decreasing trend of soil erosion areas in four provinces (e.g. Inner Mongolia, Gansu, Qinghai, and Xinjiang), especially after 2000 (Zhang et al., 2016). Secondly, a regional forest LUF increase trend occurs in the northwestern NCP (**Fig. 2c**), which agrees with the previous study of Li et al., (2016b), who reported a remarkable forest growth in the northwest of NCP from 2000 to 2010. As a result, two obvious vegetation protective barriers arise throughout in southwest to northeast direction, which is well known as "the Green Great Wall" with expectations to prevent the eastern of China from dust pollution (Parungo et al., 1994; Liu et al., 2008; Cao et al., 2011).

The land cover changes, especially the obvious vegetation growths, are mainly caused by the China's national ERPs. (1) The grassland increase is mainly induced by the desertification control programs of the "Desertification Combating around Beijing and Tianjin (DCBT)" and " the Shelterbelt Network Development Program (SNDP)". They share with the goal of dust control, planning to protect grasslands and to convert the desertified land into forestland and grassland. (2) The forest increase can be attributed to many national afforestation programs, such as the "Natural Forest Protection Program (NEPP)", "Grain for Green Project", "Three Norths Shelter Forest System Project" and so on. The China's State Forestry Administration presented enthusiasm to plant trees in the ecological restoration (Yin and Yin, 2010; Cao et al., 2011).

3.2 Model performance

The hourly measurements of [PMC] in both the dust source region (DSR) and the downward populated region (NCP region) were used to validate the WRF-DUST model simulations. **Figure 3** presents the diurnal variations of calculated and observed near-surface [PMC] averaged over the ambient monitoring site in provinces within DSR and NCP. The model reasonably well reproduces the temporal variations of surface [PMC] compared to the observations. e.g. the dust storm outbreak with peak [PMC] in DSR are reasonably earlier than that in the downwind NCP areas. The peak [PMC] occurred on 4 March within DSR (**Fig. 3a**), whereas occurred on 5 March within NCP (**Fig. 3b**). In the DSR region, the calculated results show a same phase of the peak value compared with the measured peak on 4 March. However, the calculated peak values show some underestimates of the measured value. In the NCP region, the calculated results show a same phase of the peak value compared with the measured peak on 5 March. The calculated peak value is similar to the measured peak. However, after the peak value (after 6th March), the calculated results underestimate of the measured value.

In the different provinces of the dust source region, the hourly provincial average [PMC] can exceed 500 μg m^{-3} in Ningxia, Gansu, and Inner Mongolia (the locations of these provincial average show in **Fig. 1b**) before 20:00 4th March, implicating dust storm outbreak in DSR. In the different provinces of the downward region, the peak values have time-lags (hours to half day) compared to the peak values in DSR. For example, the peak [PMC] arose first in Beijing with a time-lag of 7 hours. In other four provinces of NCP (the locations of these provincial average show in Fig. 1b), the time-lags are about 12 hours (**Fig. 3b**).

The statistical results show that the model generally exhibits good performance in simulating [PMC] in the DSR region, involving IOA of 0.96 and NMB of 2% for DSR. For the related provinces, all the IOAs exceed 0.85 and absolute NMB are lower than 13% (**Fig. 3a1–5**). The model also generally reproduces the observed [PMC] in NCP, with IOA of 0.83 for NCP and IOAs exceeding 0.67 for related provinces. However, the model biases still exist, considerably underestimation biases occurred on 6–7 March in NCP. The model underestimates considerably the observed [PMC] with average NMB of -15% in NCP (**Fig. 3b0**). And the model cannot well predict the observed [PMC] in Tianjin (**Fig. 3b2**), which is affected by the sea breeze when the large-scale wind fields are weak (**Fig. 5e, 5h**). In general, however, current numerical weather prediction models, even in research mode, still have difficulties in producing the location, timing, depth, and intensity of the sea-breeze front (Banta et al., 2005; Wang et al., 2013). The model reasonable predicts the [PMC] variations in other four provinces in NCP, with IOAs more than 0.77, but with underestimation of MBs varying from -25% to -3% (**Fig. 3b1, b3–5**), showing model biases in modeling precipitation processes.

The episode-averaged calculation was compared with the measured result in **Fig. 4.** Figure 4a provides the horizontal distributions of the simulated and the observed near-surface [PMC], along with the simulated wind fields. The WRF-DUST model reasonably reproduces spatial variation of [PMC] during the dust episode. The model simulation is also able to provide a more detailed horizontal distribution, while the measured data is generally lack of the data in the remote desert area (see **Fig. 4a**). The correlation coefficient (R) between the simulations and observations is 0.77 (see **Fig. 4b**), suggesting that the model simulation is able to represent the measured result during the dust episode period.

In order to evaluate the detailed temporal evolution of the dust plume, the daily average calculated and measured dust distributions are shown in **Fig. 5**. On 2 March, it was a starting dust storm stage, and both the observed and simulated [PMC] reached as high as 200–300 μg m^{-3} in the upwind DSR region, while in the downwind NCP region, the concentrations of [PMC] were low, being only 20–50 μg m^{-3} (**Fig 5a**). On 3 March, the dust storm was strengthened in the upwind DSR region (**Fig 5b**). On 4 March, the dust storm was further strengthened in the upwind DSR region. The area of the dust storm in DSR was enlarged, and the concentrations of [PMC] were the highest values of the episode, reaching to 300–500 μg m^{-3}. In addition, there were strong northwest winds (> 10 m s^{-1}). Due to the strong northwest prevailing winds, the dust storm started to be transported from upwind DSR to downwind NCP with northwest to southeast direction (**Fig 5c**). On 5 March, due to the strong northwest prevailing winds in the previous day, the dust storm reached to the NCP region, and caused a remarkable [PMC] increase, with the concentrations rise to 100–200 μg m^{-3}. At the same time, the dust plume was dispersed in DSR, showing a significant decrease in [PMC]. The model results well represented these important feathers (**Fig 5d**). On 6–7 March, the dust storm passed through and the wind speed slowed down, the [PMC] significantly decreased in both the DSR and NCP regions (**Fig. 5e-f**). The correlation coefficients between measured and simulated [PMC] are 0.58–0.90 in starting stage of the dust storm (**Fig. 5a-5c**), and 0.62 – 0.73 in the later stage of the dust storm (**Fig. 5d-5f**).

Generally, the WRF-DUST model well captures the spatial variations and temporal evolutions of dust storm during the episode. However, some model biases exist. For example, the model underestimates the observed [PMC] in NCP, especially during the later stage of the episode on 6–7 March (**Fig. 5e-f**), suggesting that several bias in the model (such as the bias in meteorological simulation, a faster deposition, etc.) (Bian et al., 2011; Duan et al., 2011; Bei et al., 2012).

3.3 Effect of ecological restoration on dust pollution

The evaluation the model simulation during dust storm episode suggests that the WRF-DUST model is able to simulate the dust transport from the source region to downwind areas, which can be used to assess the effect of ecological restoration on the dust pollution in the populated region, such as NCP.

Despite the ongoing debate about effectiveness (Jiang, 2005; Liu et al., 2008; Wang et al., 2010; Tan and Li, 2015; Deng et al., 2016), there are incontestably great changes of the surface properties induced by the China's national ERPs (Yin and Yin, 2010; Cao et al., 2011; Duan et al., 2011). We conducted model sensitivity studies to quantitatively evaluate the impacts of the land cover changes on the dust pollution in NCP. Two model simulations were performed. In the base case, the MCD12Q1 product with IGBP scheme in 2013 was utilized to represent the land cover situations after the ERPs. Compared with the base simulation, another simulation was conducted with same configuration and input data, except the land cover situations assimilated from the MCD12Q1 product with IGBP scheme in 2001. This model simulation represents the land cover situations without the effects of ERPs. The differences of the two model simulations of dust concentrations were compared.

Figure 6 presents the near-surface [PMC] change from 2001 to 2013, including the temporal variations and the episode-average spatial variations. The vegetation increase regions and downwind areas denoted the most remarkable change with [PMC] reduction exceeding 20%, especially for the areas where barren converted to grassland (**Fig. 2a, 2b, Fig. 6b, 6d**). The ERPs generally reduce the dust pollution in NCP during the dust storm episode, except in Henan province. The episode-average [PMC] reduction is -10% to -2% in the heart of NCP (BTH; Beijing, Tianjin, and Hebei) and Shandong. In northern Hebei, the episode-reduce [PMC] can reach as high as -20% to -10% (**Fig. 6b, 6d**). The changes of [PMC] are generally negative, implicating the effectiveness of ERPs in preventing the dust pollution in NCP, especially for BTH. During the episode when the dust storm was transported from the DSR to NCP, the benefits of ERPs induced dust pollution reduction are remarkable, with the reduction of [PMC] ranging -5% to -15% in NCP. The highest reduction of [PMC] induced by ERPs are -15.3% (-21.0 μg m^{-3}) for BTH and -6.2% (-9.34 μg m^{-3}) for NCP (**Fig 6a, 6c**).

Figure 7 shows the detailed horizontal distributions in the different stages of the episode, such as T1 (08:00, 4 March), T2 (02:00, 5 March), T3 (13:00 5 March), and

Atmos. Chem. Phys. Discuss., https://doi.org/10.5194/acp-2017-855
Manuscript under review for journal Atmos. Chem. Phys.
Discussion started: 27 October 2017

Atmospheric Chemistry and Physics
Open Access
Discussions

T4 (04:00, 6 March). T1 and T2 are at the time points of dust outbreak in DSR, while the T3 and T4 are at time points of dust pollutants being transported to NCP. All of the four key time points correspond to peak [PMC] change (**Fig 6a, 6c**). To capture different dust pollution phases, we analyzed the [PMC] change distributions for these time points (**Fig. 7**). At T1, the dust storm started and was limited in DSR (**Fig. 7a**). Hence, ERPs caused prominent [PMC] decrease in DSR (-16.7 μg m^{-3}), whereas had small influence in NCP (lower than 2.0 μg m^{-3} both in NCP and BTH) (**Fig. 6a, Fig. 7b**). At T2, dust storm was transported from DSR to NCP. As a result, the [PMC] values were diluted in DSR, while were enhanced in NCP (**Fig. 7c**). [PMC] decrease was considerable in DSR (-8.0 μg m^{-3}), and there was a significant [PMC] decrease in northern NCP by about -10.0 to -30.0 μg m^{-3} (**Fig. 7d)**. At T3, the dust storm moved from the source region to the downwind NCP region (**Fig. 7e**). The ERPs significantly reduced the dust pollution in the NCP region (**Fig. 7f**), causing the remarkable [PMC] reduction in BTH (-19.3 μg m^{-3}) and NCP (-9.3 μg m^{-3}) (**Fig. 6a, 6c**). At T4, it was the point of the end of the dust episode, and the [PMC] values wee started to decrease (**Fig. 7g**).

4 Summary and conclusions

Dust pollution has significant impacts on human's life in China, especially in springtime. To reduce dust pollution problem, Chinese government has taken great efforts for initiating national ecological restoration programs (ERPs) since 1978. Despite the incontestably great changes of surface properties induced by ERPs, the effectiveness of ERPs in dust pollution control is not well understood. In the present study, we are trying to assess the impact of ERPs on the dust pollutions, especially in the downwind populated region (NCP). First, the ERPs induced land cover changes are investigated, using the long-term satellite measurements. The gridded LUF matrixes are calculated and then assimilated, which can provide more accurate surface properties than previous studies, especially for the dust emissions due to wind erosion in the WRF-DUST model. Second, the WRF-DUST model is applied to evaluate the effects of the ERPs on the dust pollution control in NCP. Some important results are summarized as follows:

1. A more detailed land surface properties are quantified by calculating gridded LUF

Atmos. Chem. Phys. Discuss., https://doi.org/10.5194/acp-2017-855
Manuscript under review for journal Atmos. Chem. Phys.
Discussion started: 27 October 2017

based on long-term satellite measurement. Two important vegetation (grass and forest) are increased in berried lands and deserts in northwestern China, which locate in the upwind regions of the populated areas of NCP in eastern China. As a result, China has impressive progress in implementing some of the world's largest ERPs, which could produce important impacts on the dust pollution in eastern of China.

2. The WRF-DUST model is applied to assess the effect of ERPs on dust pollutions. The model calculations are intensively evaluated. Despite some model biases, the WRF-DUST model reasonably reproduced the temporal and spatial dust pollution episode both in upwind DSR and downwind NCP regions, especially for the dust storm outbreak and the down wind transport. The correlation coefficients (R) between simulated and observed [PMC] are 0.96 for DSR and 0.83 for NCP, and the NMBs are 2% and -15%, respectively.

3. The impacts of EPRs induced land cover changes on the dust pollution in NCP are assessed during an episode of dust storm (from 02 to 07 March, 2016). The results suggest that ERPs significantly reduce the dust pollution in NCP, especially in the heart area of NCP (BTH). During the episode when the dust storm was transported from the DSR to NCP, the reduction of dust pollution induced by ERPs ranges from -5% to -15% in NCP, with the maximum reduction of -15.3% (-21.0 μg m^{-3}) in BTH, and -6.2% (-9.3 μg m^{-3}) in NCP.

The air pollution is severe in eastern China, especially in NCP, and the dust pollutions have important contributions to the severe air pollutions. This study shows that ERPs help to reduce some air pollutions in the region, especially in springtime, suggesting the important contribution of ERPs to the air pollution control in China. It should be reiterated that, considering the limitation of case study and the sparse empirical evidence, the main focus of this study does not intent to give a general conclusion, but rather to provide some insights of the effect of ERPs on the downwind area, where heavy haze often occurred due to anthropogenic air pollutants.

Acknowledgement

This work is supported by the National Natural Science Foundation of China (NSFC) under Grant No. 41430424 and 41375136, and the China Postdoctoral Science Foundation under Grant No. 2016M602886. This work is also supported by the Fundamental Research Funds for the Central Universities. The National Center for Atmospheric Research is sponsored by the National Science Foundation.

Reference

Banta, R., Senff, C., Nielsen-Gammon, J., Darby, L., Ryerson, T., Alvarez, R., Sandberg, S., Williams, E., and Trainer, M.: A bad air day in Houston, Bulletin of the American Meteorological Society, 86, 657-669, 2005.

Bei, N., Li, G., and Molina, L.: Uncertainties in SOA simulations due to meteorological uncertainties in Mexico City during MILAGRO-2006 field campaign, Atmospheric Chemistry and Physics, 12, 11295, 2012.

Bian, H., Tie, X.-X., Cao, J.-J., Ying, Z. M., Han, S.-Q., and Xue, Y.: Analysis of a severe dust storm event over China: Application of WRF-dust model, 2011.

Cao, S., Chen, L., Shankman, D., Wang, C., Wang, X., and Zhang, H.: Excessive reliance on afforestation in China's arid and semi-arid regions: Lessons in ecological restoration, Earth-Science Reviews, 104, 240-245, 2011.

Chen, F., and Dudhia, J.: Coupling an advanced land surface–hydrology model with the Penn State–NCAR MM5 modeling system. Part II: Preliminary model validation, Monthly Weather Review, 129, 587-604, 2001.

Chin, M., Rood, R. B., Lin, S. J., Müller, J. F., and Thompson, A. M.: Atmospheric sulfur cycle simulated in the global model GOCART: Model description and global properties, Journal of Geophysical Research: Atmospheres, 105, 24671-24687, 2000.

Cottle, P., Strawbridge, K., McKendry, I., O'Neill, N., and Saha, A.: A pervasive and persistent Asian dust event over North America during spring 2010: lidar and sunphotometer observations, Atmospheric Chemistry and Physics, 13, 4515, 2013.

Deng, L., Yan, W., Zhang, Y., and Shangguan, Z.: Severe depletion of soil moisture following land-use changes for ecological restoration: Evidence from northern China, Forest Ecology and Management, 366, 1-10, 2016.

Duan, H., Yan, C., Tsunekawa, A., Song, X., Li, S., and Xie, J.: Assessing vegetation dynamics in the Three-North Shelter Forest region of China using AVHRR NDVI data, Environmental Earth Sciences, 64, 1011-1020, 2011.

Evan, A. T., Heidinger, A. K., Bennartz, R., Bennington, V., Mahowald, N. M., Corrada‐Bravo, H., Velden, C. S., Myhre, G., and Kossin, J. P.: Ocean temperature forcing by aerosols across the Atlantic tropical cyclone development region, Geochemistry, Geophysics, Geosystems, 9, 2008.

Fan, K., Xie, Z., Wang, H., Xu, Z., and Liu, J.: Frequency of spring dust weather in North China linked to sea ice variability in the Barents Sea, Climate Dynamics, 1-12, 2017.

Friedl, M. A., McIver, D. K., Hodges, J. C., Zhang, X., Muchoney, D., Strahler, A. H., Woodcock, C. E., Gopal, S., Schneider, A., and Cooper, A.: Global land cover mapping from MODIS: algorithms and early results, Remote Sensing of Environment, 83, 287-302, 2002.

Friedl, M. A., Sulla-Menashe, D., Tan, B., Schneider, A., Ramankutty, N., Sibley, A., and Huang, X.: MODIS Collection 5 global land cover: Algorithm refinements and characterization of new datasets, Remote sensing of Environment, 114, 168-182, 2010.

Fu, J. S.: Model development of dust emission and heterogeneous chemistry within the Community Multiscale Air Quality modeling system and its application over East Asia, Atmospheric Chemistry and Physics, 16, 8157, 2016.

Gerten, D., Schaphoff, S., Haberlandt, U., Lucht, W., and Sitch, S.: Terrestrial vegetation and water balance—hydrological evaluation of a dynamic global vegetation model, Journal of Hydrology, 286, 249-270, 2004.

Giannadaki, D., Pozzer, A., and Lelieveld, J.: Modeled global effects of airborne desert dust on air quality and premature mortality, Atmospheric Chemistry and Physics, 14, 957-968, 2014.

Ginoux, P., Chin, M., Tegen, I., Prospero, J. M., Holben, B., Dubovik, O., and Lin, S. J.: Sources and distributions of dust aerosols simulated with the GOCART model, Journal of Geophysical Research: Atmospheres, 106, 20255-20273, 2001.

Grell, G. A., Peckham, S. E., Schmitz, R., McKeen, S. A., Frost, G., Skamarock, W. C., and Eder, B.: Fully coupled "online" chemistry within the WRF model, Atmospheric Environment, 39, 6957-6975, 2005.

Grini, A., Myhre, G., Zender, C. S., and Isaksen, I. S.: Model simulations of dust sources and transport in the global atmosphere: Effects of soil erodibility and wind speed variability, Journal of Geophysical

Research: Atmospheres, 110, 2005.

Guenther, C.: Estimates of global terrestrial isoprene emissions using MEGAN (Model of Emissions of Gases and Aerosols from Nature), Atmospheric Chemistry and Physics, 6, 2006.

Haywood, J. M., Allan, R. P., Culverwell, I., Slingo, T., Milton, S., Edwards, J., and Clerbaux, N.: Can desert dust explain the outgoing longwave radiation anomaly over the Sahara during July 2003?, Journal of Geophysical Research: Atmospheres, 110, 2005.

Ho, K., Lee, S., Chan, C. K., Jimmy, C. Y., Chow, J. C., and Yao, X.: Characterization of chemical species in PM 2.5 and PM 10 aerosols in Hong Kong, Atmospheric Environment, 37, 31-39, 2003.

Hong, S.-Y., and Lim, J.-O. J.: The WRF single-moment 6-class microphysics scheme (WSM6), J. Korean Meteor. Soc, 42, 129-151, 2006.

Janić, Z. I.: Nonsingular implementation of the Mellor-Yamada level 2.5 scheme in the NCEP Meso model, US Department of Commerce, National Oceanic and Atmospheric Administration, National Weather Service, National Centers for Environmental Prediction, 2001.

Jiang, G.: It is inappropriate for afforestation in the "Three North" regions, Sci. Decis. Making, 11, 40-42, 2005.

Jickells, T., An, Z., Andersen, K. K., Baker, A., Bergametti, G., Brooks, N., Cao, J., Boyd, P., Duce, R., and Hunter, K.: Global iron connections between desert dust, ocean biogeochemistry, and climate, science, 308, 67-71, 2005.

Kang, C.-H., Kim, W.-H., Ko, H.-J., and Hong, S.-B.: Asian dust effects on total suspended particulate (TSP) compositions at Gosan in Jeju Island, Korea, Atmospheric Research, 94, 345-355, 2009.

Lee, E.-H., and Sohn, B.-J.: Recent increasing trend in dust frequency over Mongolia and Inner Mongolia regions and its association with climate and surface condition change, Atmospheric Environment, 45, 4611-4616, 2011.

Li, H., Yang, X., Zhao, Y., Wang, M., and Huo, W.: The atmospheric circulation patterns influencing the frequency of spring sand-dust storms in the Tarim Basin, Sciences in Cold and Arid Regions, 6, 168-173, 2014.

Li, N., Long, X., Tie, X., Cao, J., Huang, R., Zhang, R., Feng, T., Liu, S., and Li, G.: Urban dust in the Guanzhong basin of China, part II: A case study of urban dust pollution using the WRF-Dust model, Science of The Total Environment, 541, 1614-1624, 2016a.

Li, X., Wang, H., Zhou, S., Sun, B., and Gao, Z.: Did ecological engineering projects have a significant effect on large-scale vegetation restoration in Beijing-Tianjin Sand Source Region, China? A remote sensing approach, Chinese geographical science, 26, 216, 2016b.

Liao, H., Seinfeld, J. H., Adams, P. J., and Mickley, L. J.: Global radiative forcing of coupled tropospheric ozone and aerosols in a unified general circulation model, Journal of Geophysical Research: Atmospheres, 109, 2004.

Liu, J., Li, S., Ouyang, Z., Tam, C., and Chen, X.: Ecological and socioeconomic effects of China's policies for ecosystem services, Proceedings of the National academy of Sciences, 105, 9477-9482, 2008.

Lou, S., Liao, H., and Zhu, B.: Impacts of aerosols on surface-layer ozone concentrations in China through heterogeneous reactions and changes in photolysis rates, Atmospheric environment, 85, 123-138, 2014.

Lu, C., Zhao, T., Shi, X., and Cao, S.: Ecological restoration by afforestation may increase groundwater depth and create potentially large ecological and water opportunity costs in arid and semiarid China, Journal of Cleaner Production, 2016.

Lü, Y., Zhang, L., Feng, X., Zeng, Y., Fu, B., Yao, X., Li, J., and Wu, B.: Recent ecological transitions in China: greening, browning, and influential factors, Scientific reports, 5, 2015.

Moulin, C., Lambert, C. E., Dulac, F., and Dayan, U.: Control of atmospheric export of dust from North Africa by the North Atlantic Oscillation, Nature, 387, 691, 1997.

Park, S. U., and In, H. J.: Parameterization of dust emission for the simulation of the yellow sand (Asian dust) event observed in March 2002 in Korea, Journal of Geophysical Research: Atmospheres, 108, 2003.

Parungo, F., Li, Z., Li, X., Yang, D., and Harris, J.: Gobi dust storms and the Great Green Wall, Geophysical research letters, 21, 999-1002, 1994.

Peng, S., Chen, A., Xu, L., Cao, C., Fang, J., Myneni, R. B., Pinzon, J. E., Tucker, C. J., and Piao, S.: Recent change of vegetation growth trend in China, Environmental Research Letters, 6, 044027, 2011.

Piao, S., Fang, J., Zhou, L., Guo, Q., Henderson, M., Ji, W., Li, Y., and Tao, S.: Interannual variations of monthly and seasonal normalized difference vegetation index (NDVI) in China from 1982 to 1999, Journal of Geophysical Research: Atmospheres, 108, 2003.

Qian, W., Quan, L., and Shi, S.: Variations of the dust storm in China and its climatic control, Journal of Climate, 15, 1216-1229, 2002.

Atmos. Chem. Phys. Discuss., https://doi.org/10.5194/acp-2017-855
Manuscript under review for journal Atmos. Chem. Phys.
Discussion started: 27 October 2017

Atmospheric Chemistry and Physics
Open Access
EGU
Discussions

Reichstein, M., Ciais, P., Papale, D., Valentini, R., Running, S., Viovy, N., Cramer, W., Granier, A., Ogee, J., and Allard, V.: Reduction of ecosystem productivity and respiration during the European summer 2003 climate anomaly: a joint flux tower, remote sensing and modelling analysis, Global Change Biology, 13, 634-651, 2007.

Rosenfeld, D., Rudich, Y., and Lahav, R.: Desert dust suppressing precipitation: A possible desertification feedback loop, Proceedings of the National Academy of Sciences, 98, 5975-5980, 2001.

Shen, Z., Cao, J., Liu, S., Zhu, C., Wang, X., Zhang, T., Xu, H., and Hu, T.: Chemical composition of PM10 and PM2. 5 collected at ground level and 100 meters during a strong winter-time pollution episode in Xi'an, China, Journal of the Air & Waste Management Association, 61, 1150-1159, 2011.

Sun, Y., Zhuang, G., Wang, Y., Zhao, X., Li, J., Wang, Z., and An, Z.: Chemical composition of dust storms in Beijing and implications for the mixing of mineral aerosol with pollution aerosol on the pathway, Journal of Geophysical Research: Atmospheres, 110, 2005.

Tan, M., and Li, X.: Does the Green Great Wall effectively decrease dust storm intensity in China? A study based on NOAA NDVI and weather station data, Land Use Policy, 43, 42-47, 2015.

Turner, B. L., Lambin, E. F., and Reenberg, A.: The emergence of land change science for global environmental change and sustainability, Proceedings of the National Academy of Sciences, 104, 20666-20671, 2007.

Wang, G., Innes, J. L., Lei, J., Dai, S., and Wu, S. W.: China's forestry reforms, Science, 318, 1556-1557, 2007.

Wang, J., Ge, C., Yang, Z., Hyer, E. J., Reid, J. S., Chew, B.-N., Mahmud, M., Zhang, Y., and Zhang, M.: Mesoscale modeling of smoke transport over the Southeast Asian Maritime Continent: Interplay of sea breeze, trade wind, typhoon, and topography, Atmospheric Research, 122, 486-503, 2013.

Wang, Q., Zhuang, G., Li, J., Huang, K., Zhang, R., Jiang, Y., Lin, Y., and Fu, J. S.: Mixing of dust with pollution on the transport path of Asian dust—Revealed from the aerosol over Yulin, the north edge of Loess Plateau, Science of the total environment, 409, 573-581, 2011.

Wang, R., Liu, B., Li, H., Zou, X., Wang, J., Liu, W., Cheng, H., Kang, L., and Zhang, C.: Variation of strong dust storm events in Northern China during 1978–2007, Atmospheric Research, 183, 166-172, 2017.

Wang, X., Zhang, C., Hasi, E., and Dong, Z.: Has the Three Norths Forest Shelterbelt Program solved the desertification and dust storm problems in arid and semiarid China?, Journal of Arid Environments, 74, 13-22, 2010.

Atmos. Chem. Phys. Discuss., https://doi.org/10.5194/acp-2017-855
Manuscript under review for journal Atmos. Chem. Phys.
Discussion started: 27 October 2017

Atmospheric Chemistry and Physics Discussions

Wang, X., Hua, T., Zhang, C., Lang, L., and Wang, H.: Aeolian salts in Gobi deserts of the western region of Inner Mongolia: Gone with the dust aerosols, Atmospheric research, 118, 1-9, 2012.

Watanabe, M., Kurai, J., Tomita, K., Sano, H., Abe, S., Saito, R., Minato, S., Igishi, T., Burioka, N., and Sako, T.: Effects on asthma and induction of interleukin-8 caused by Asian dust particles collected in western Japan, Journal of Asthma, 51, 595-602, 2014.

Yin, R., and Yin, G.: China's primary programs of terrestrial ecosystem restoration: initiation, implementation, and challenges, Environmental management, 45, 429-441, 2010.

Yoon, J. E., Kim, K., Macdonald, A. M., Park, K. T., Kim, H. C., Yoo, K. C., Yoon, H. I., Yang, E. J., Jung, J., and Lim, J. H.: Spatial and temporal variabilities of spring Asian dust events and their impacts on chlorophyll‐a concentrations in the western North Pacific Ocean, Geophysical Research Letters, 44, 1474-1482, 2017.

Zhang, Q., Streets, D. G., Carmichael, G. R., He, K., Huo, H., Kannari, A., Klimont, Z., Park, I., Reddy, S., and Fu, J.: Asian emissions in 2006 for the NASA INTEX-B mission, Atmospheric Chemistry and Physics, 9, 5131-5153, 2009.

Zhang, W., Hu, G., Dang, Y., Weindorf, D. C., and Sheng, J.: Afforestation and the impacts on soil and water conservation at decadal and regional scales in Northwest China, Journal of Arid Environments, 130, 98-104, 2016.

Zhao, B., Wang, S., Dong, X., Wang, J., Duan, L., Fu, X., Hao, J., and Fu, J.: Environmental effects of the recent emission changes in China: implications for particulate matter pollution and soil acidification, Environmental Research Letters, 8, 024031, 2013.

Zhou, L., Wang, W., Ge, M., and Tong, S.: Heterogeneous uptake of gaseous hydrogen peroxide on mineral dust, Journal of Environmental Sciences, 40, 44-50, 2016.

Atmos. Chem. Phys. Discuss., https://doi.org/10.5194/acp-2017-855
Manuscript under review for journal Atmos. Chem. Phys.
Discussion started: 27 October 2017

Atmospheric Chemistry and Physics
Discussions

Figure Captions

Figure 1. WRF-DUST simulation domain with surface land properties and major natural dust sources in China. The crosses represent centers with ambient monitoring sites. The land cover properties are derived from the MCD12Q1 product in the year 2013. Distribution of Gobi and deserts are adapted from 1:200,00 desert distribution dataset provide by the Environmental and Ecological Science Data Center for West China, National Natural Science Foundation of China (http://westdc.westgis.ac.cn).

Figure 2. The horizontal distributions of land cover changes induced by the ERPs from 2001 to 2013 for the categories of **(a)** barrens, **(b)** grasslands/savannas, **(c)** forest, and **(d)** others.

Figure 3. The temporal variations of predicted (read lines) and observed (black dots) diurnal profiles of near-surface [PMC] over all ambient monitoring stations in provinces within regions of DSR and NCP. The model performance statistics of *NMB*, and *IOA* are also shown. The x-axis is the date in Beijing Time.

Figure 4. The comparison of calculated (color contour) and observed (colored circles) episode average [PMC]. (**a**) [PMC] distribution along with the simulated wind fields (black arrows). (**b**) The correlation analysis.

Figure 5. The distribution of calculated (color contour) and observed (colored circles) daily average [PMC], along with the simulated wind fields (black arrows). The correlation indices (R) between measurements and simulations are also presented.

Figure 6. The impacts of ERPs on near-surface [PMC] in regions of DSR, NCP and BTH, including (**a, c**) the temporal variations and (**b, d**) the episode-average spatial variations. Both the concentration (**a, b**) and percentage (**c, d**) influences are presented.

Figure 7. The horizontal distributions of (**a, c, e, g**) [PMC] and (**b, d, f, h**) [PMC] change for the key time points of T1, T2, T3, and T4 (see Fig. 6). The pattern comparisons of simulated vs. observed [PMC] are shown in left panels, as well as their correlation indices, along with the simulated wind field.

Atmos. Chem. Phys. Discuss., https://doi.org/10.5194/acp-2017-855
Manuscript under review for journal Atmos. Chem. Phys.
Discussion started: 27 October 2017

Atmospheric Chemistry and Physics
Open Access
Discussions

Figure 1

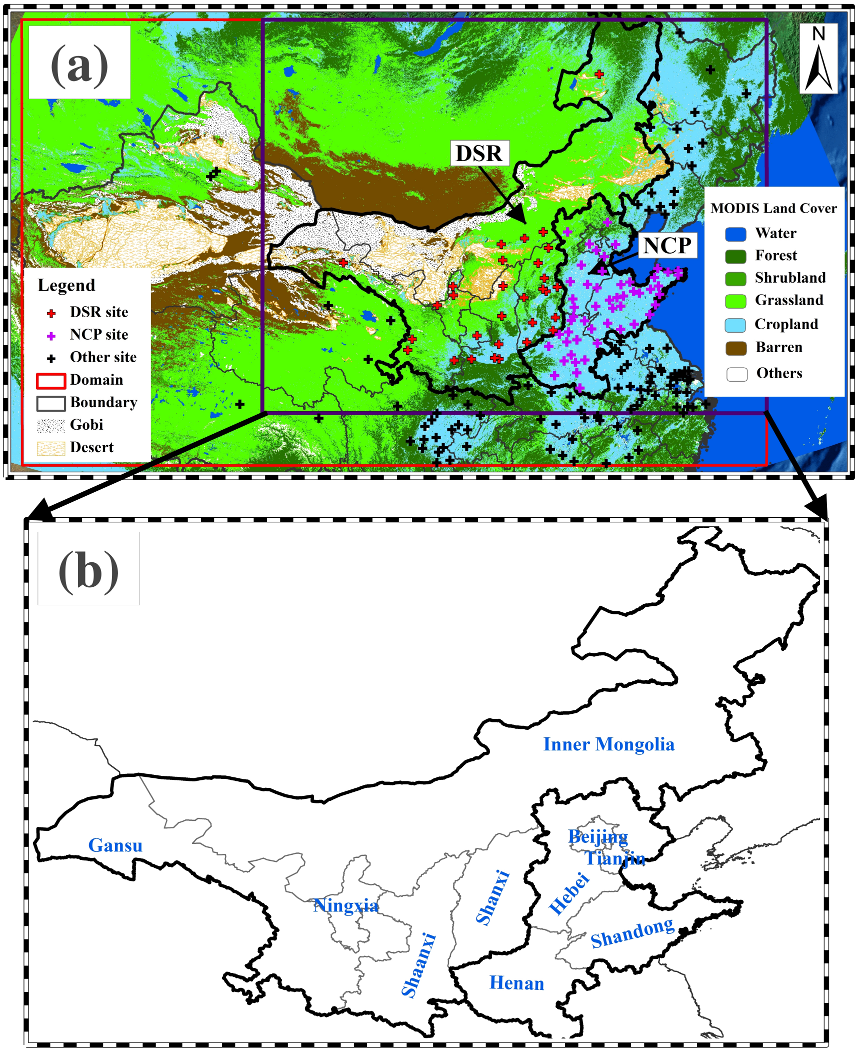

Figure 1. **(a)** WRF-DUST simulation domain with surface land properties and major natural dust sources in China. **(b)** The details of ROIs for the dust source region and surrounding areas (DSR) and the downwind North China Plain (NCP) region. The crosses represent centers with ambient monitoring sites. The land cover properties are derived from the MCD12Q1 product in the year 2013. Distribution of Gobi and deserts are adapted from 1:200,00 desert distribution dataset provide by the Environmental and Ecological Science Data Center for West China, National Natural Science Foundation of China (http://westdc.westgis.ac.cn). The DSR region contains five provinces in the northwest of NCP, involving Ningxia, Gansu, Shanxi, Inner Mongolia and Shanxi. The NCP includes five provinces of the Beijing, Tianjin, Hebei, Henan and Shandong.

Atmos. Chem. Phys. Discuss., https://doi.org/10.5194/acp-2017-855
Manuscript under review for journal Atmos. Chem. Phys.
Discussion started: 27 October 2017

Figure 2

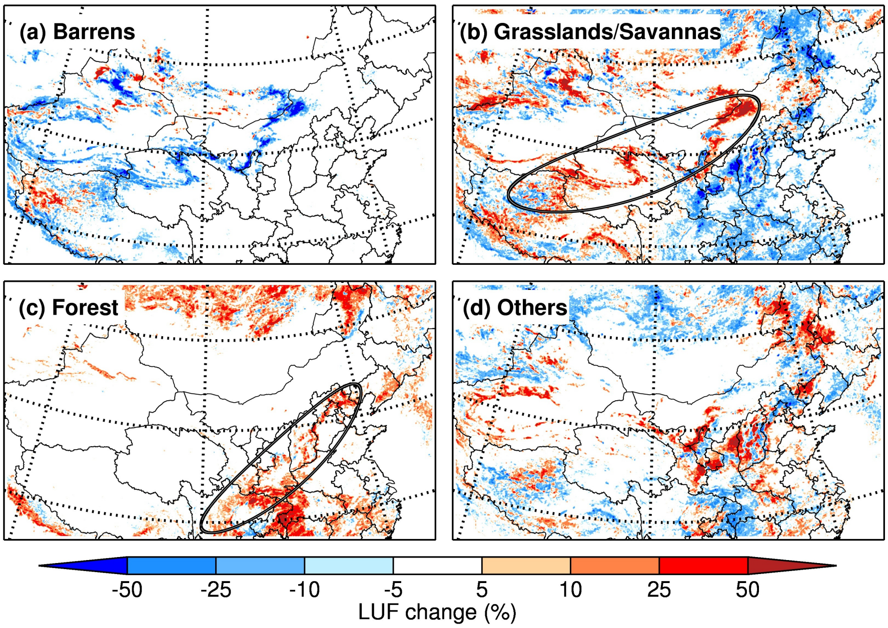

Figure 2. The horizontal distributions of land cover changes induced by the ERPs from 2001 to 2013 for the categories of **(a)** barrens, **(b)** grasslands/savannas, **(c)** forest, and **(d)** others.

Atmos. Chem. Phys. Discuss., https://doi.org/10.5194/acp-2017-855
Manuscript under review for journal Atmos. Chem. Phys.
Discussion started: 27 October 2017

Atmospheric Chemistry and Physics
Discussions

Figure 3

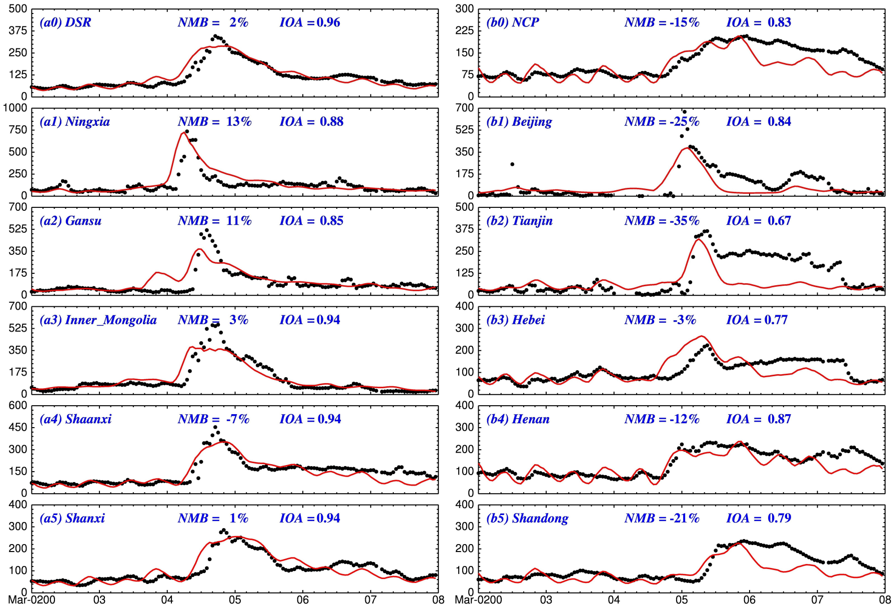

Figure 3. The temporal variations of predicted (read lines) and observed (black dots) diurnal profiles of near-surface [PMC] over all ambient monitoring stations in provinces within regions of DSR and NCP. The model performance statistics of *NMB*, and *IOA* are also shown. The x-axis is the date in Beijing Time.

Atmos. Chem. Phys. Discuss., https://doi.org/10.5194/acp-2017-855
Manuscript under review for journal Atmos. Chem. Phys.
Discussion started: 27 October 2017

Figure 4

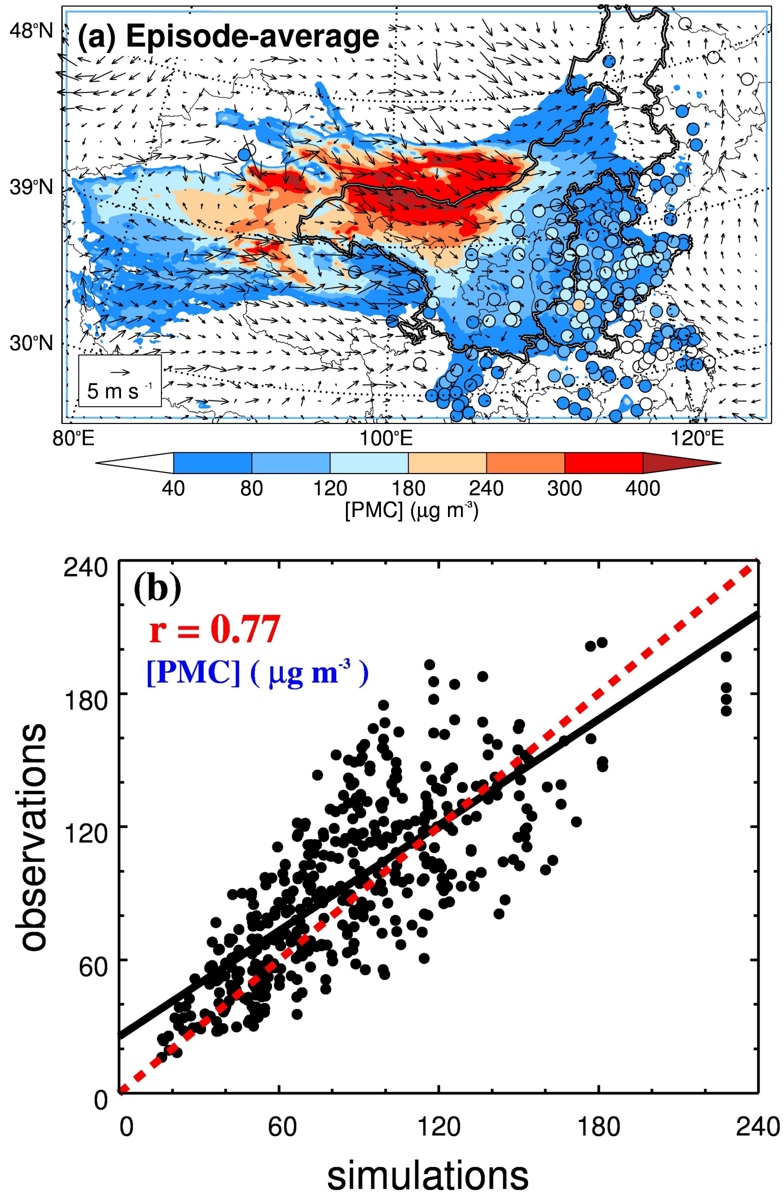

Figure 4. The comparison of calculated (color contour) and observed (colored circles) episode average [PMC]. (**a**) [PMC] distribution along with the simulated wind fields (black arrows). (**b**) The correlation analysis.

Atmos. Chem. Phys. Discuss., https://doi.org/10.5194/acp-2017-855
Manuscript under review for journal Atmos. Chem. Phys.
Discussion started: 27 October 2017

Figure 5

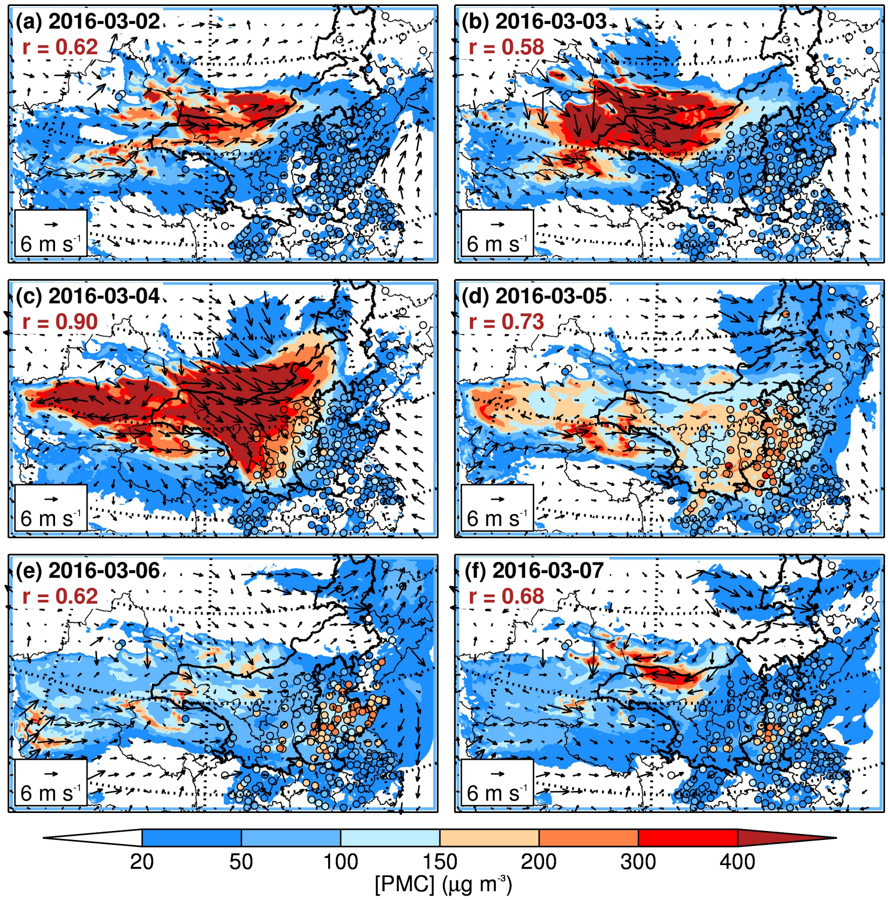

Figure 5. The distribution of calculated (color contour) and observed (colored circles) daily average [PMC], along with the simulated wind fields (black arrows). The correlation indices (R) between measurements and simulations are also presented.

Atmos. Chem. Phys. Discuss., https://doi.org/10.5194/acp-2017-855
Manuscript under review for journal Atmos. Chem. Phys.
Discussion started: 27 October 2017

Atmospheric Chemistry and Physics
Open Access
Discussions
EGU

Figure 6

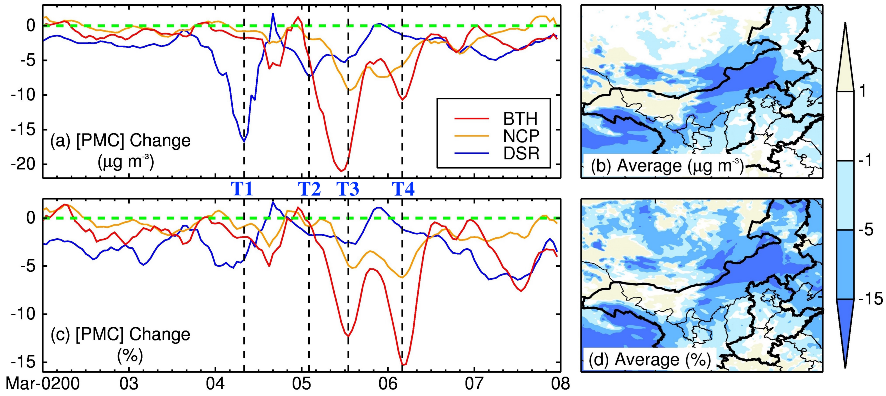

Figure 6. The impacts of ERPs on near-surface [PMC] in regions of DSR, NCP and BTH, including (**a, c**) the temporal variations and (**b, d**) the episode-average spatial variations. Both the concentration (**a, b**) and percentage (**c, d**) influences are presented.

Atmos. Chem. Phys. Discuss., https://doi.org/10.5194/acp-2017-855
Manuscript under review for journal Atmos. Chem. Phys.
Discussion started: 27 October 2017

692 **Figure 7**

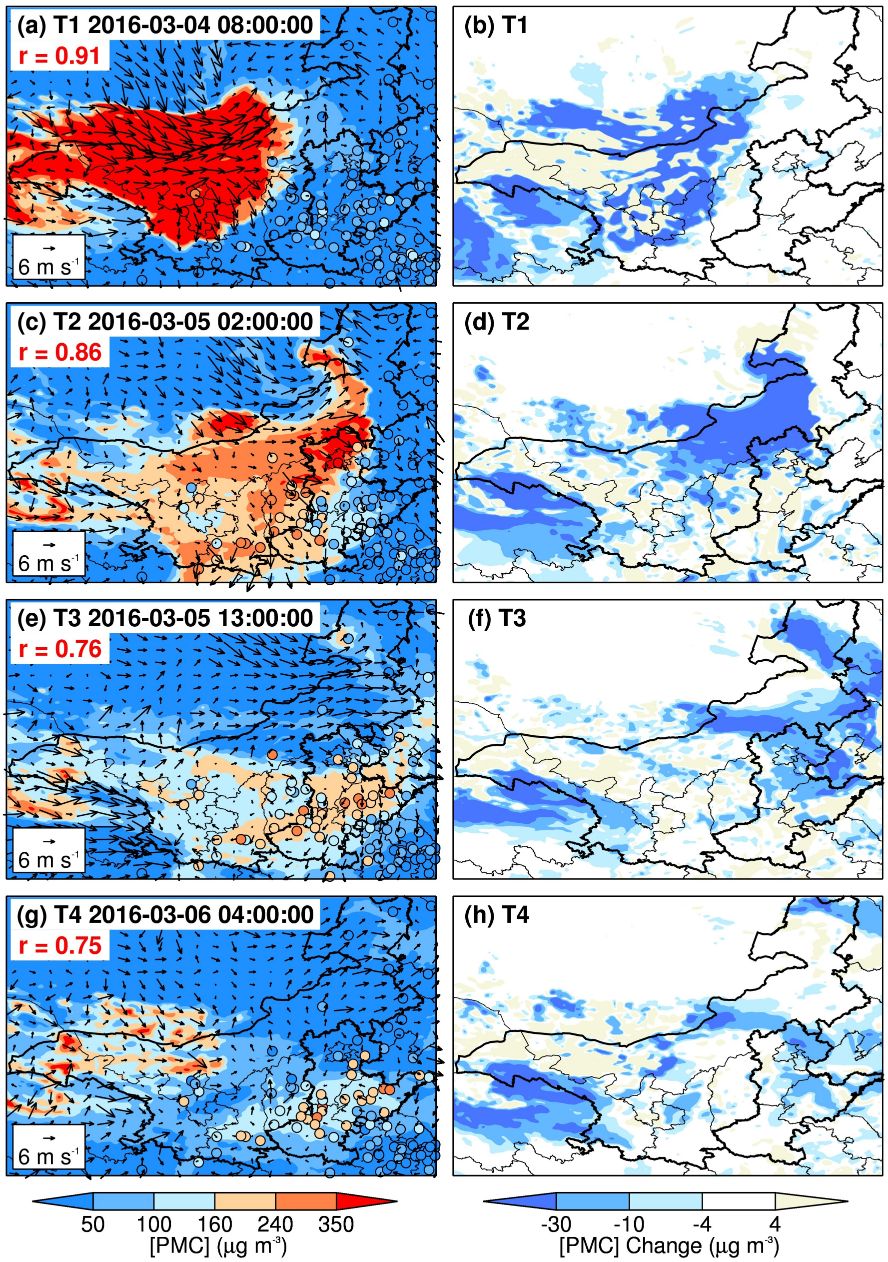

693

694 **Figure 7**. The horizontal distributions of (**a, c, e, g**) [PMC] and (**b, d, f, h**) [PMC]
695 change for the key time points of T1, T2, T3, and T4 (see Fig. 6). The pattern
696 comparisons of simulated vs. observed [PMC] are shown in left panels, as well as the
697 correlation indices, along with the simulated wind field.